DALTON
FULL PAPER

Complexes of the tripodal nitrilotrimethylenetrisphosphonic (H_6L) and *P*,*P*′,*P*″-triphenylnitrilotrimethylenetrisphosphinic ($H_3L°$) acids with the copper(II) ion. Synthesis and characterization of $[Hpy][Cu(H_3L)(H_2O)]$ and $[Cu(HL°)(py)]_2·2Me_2CO$†

Franco Cecconi,[a] Carlo A. Ghilardi,[a] Pablo A. Lorenzo Luis,[a] Stefano Midollini,[a] Annabella Orlandini,[a] Dainis Dakternieks,[b] Andrew Duthie,[b] Sixto Dominguez,[c] Elisabetta Berti[d] and Alberto Vacca[d]

[a] *Istituto per lo Studio della Stereochimica ed Energetica dei Composti di Coordinazione, CNR, Via J. Nardi 39, 50132 Firenze, Italy*
[b] *Centre for Chiral and Molecular Technologies, Deakin University, Geelong Victoria, 3217, Australia*
[c] *Departmento de Quimica Inorganica, Universidad de La Laguna, 38204, La Laguna, Tenerife, Canary Islands, Spain*
[d] *Dipartimento di Chimica, Università di Firenze, 50144 Firenze, Italy*

Received 8th June 2000, Accepted 20th November 2000

The complexes $[Hpy][Cu(H_3L)(H_2O)]$ **1** (L^{6-} = nitrilotrimethylenetrisphosphonate) and $[Cu(HL°)(py)]_2·2Me_2CO$ **2** [$(L°)^{3-}$ = *P*,*P*′,*P*″-triphenylnitrilotrismethylenetrisphosphinate)] have been isolated and characterized by X-ray crystallography, near IR-visible spectroscopy and magnetic measurements. The structure determination has shown the complexes to be constituted by monomeric and dimeric units respectively. In the monomer the metal atom is surrounded by the phosphonate ligand and a water molecule, with a geometry between a trigonal bipyramid and a square pyramid. The two copper atoms in the dimer are held together by an arm of the tripod ligand, with a pyridine molecule as additional ligand, and display octahedral geometry. The presence of monomeric and dimeric species in aqueous solutions of **1** and **2** has been shown by ESMS studies. The formation in water solution of the dimer $[\{Cu(H_3L)\}_2]^{2-}$, as a minor species, has been supported by potentiometric measurements, whereas only the monomeric anion $[CuL°]^-$ has been ascertained to be present. In general the ligand $H_3L°$ forms less stable copper(II) complexes than H_6L.

Introduction

The area of metal phosphonate chemistry has developed significantly in the last decade. Indeed these systems, owing to their aptitude to form networks of extended molecular interactions, have several potential applications in ion exchange, catalysis, magnetic studies, intercalation chemistry, *etc.*[1]

The aminopolyphosphonates have widely been used as scale inhibitors in industry and magnetic resonance image agents in medicine.[2] In comparison with the aminopolycarboxylates, the aminopolyphosphonates, in which a carboxylate CO_2^- group is replaced by a phosphonate PO_3^{2-} moiety, contain a higher number of negative charges. As a consequence the aminopolyphosphonates, unlike the aminopolycarboxylates, easily form protonated complexes.

The formation and protonation of the complexes[3] of nitrilotrimethylenetrisphosphonate (L^{6-}), Scheme 1, or related (acetate–methylenephosphonate ligands[4] and transition metal(II) ions, have widely been investigated but no crystal structures have so far been reported. Now we have synthesized the two copper(II) complexes $[Hpy][Cu(H_3L)(H_2O)]$ and $[Cu(HL°)(py)]_2·2Me_2CO$, where $(L°)^{3-}$ is the closely related tripod *P*,*P*′,*P*″-triphenylnitrilotrimethylenetrisphosphinate, Scheme 1. The complexes have been characterized through X-ray diffraction analyses, electrospray mass spectrometry (ESMS), near IR-visible spectroscopy, and magnetic measurements. Deprotonation of $H_3L°$ and formation of its copper(II) complexes, in aqueous solution, has been investigated through potentiometric measurements. The formation of complexes of copper(II) ion and H_6L has also been reinvestigated.

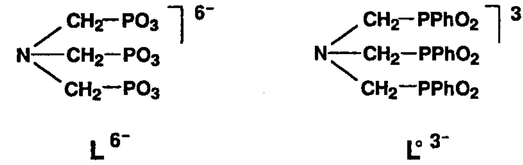

Scheme 1

Experimental

Materials and methods

All chemicals were used as received without further purification. Nitrilotrimethylenetrisphosphonic acid was purchased from Fluka. *P*,*P*′,*P*″-Triphenylnitrilotrimethylenetrisphosphinic acid was synthesized according a previously reported method.[5] The $[(CH_3)_4N]Cl$ and $[(CH_3)_4N]OH$ solutions for potentiometry were prepared from Merck products. A stock $CuCl_2$ solution was prepared from the Merck analysis grade product and standardized by complexometric titration, according to the procedure of Schwarzenbach.[6] The electronic spectra were measured with a Perkin-Elmer Lambda 9 UV/VIS/NIR spectrophotomer. The temperature dependence of the magnetic

---

† Electronic supplementary information (ESI) available: negative ion ESMS spectra of complexes **1** and **2**. See http://www.rsc.org/suppdata/dt/b0/b004576o/

DOI: 10.1039/b004576o

susceptibility was measured with a Metronique Ingenierie MS-03 SQUID magnetometer, in the range 246–3 K. The diamagnetic correction applied was 766.52 × 10^{-6} emu mol^{-1}, for the dimeric compound.

Synthesis of the complexes

[Hpy][Cu(H_3L)(H_2O)] 1. A solution of H_6L (300 mg, 1 mmol) dissolved in water–pyridine (10 ml/5 ml) was added to a solution of $Cu(O_2CCH_3)_2{\cdot}H_2O$ (200 mg, 1 mmol) in pyridine (10 ml). Then acetone (50 ml) was added dropwise and a pale blue crystalline precipitate formed over a period of 24 hours. The complex was filtered off, washed with acetone and then dried *in vacuo*. The product was dissolved in water (15 ml) and by slow diffusion of acetone (35 ml) through the solution well shaped crystals precipitated. Yield 370 mg, 80% (Found: C, 20.90; H, 3.68; N, 6.00. Calc. for $C_8H_{17}CuN_2O_{10}P_3$: C, 20.99; H, 3.75; N, 6.12%).

[Cu(HL°)(py)]$_2$·2Me$_2$CO 2. A solution of $H_3L°$ (480 mg, 1 mmol) in pyridine (15 ml) was added to a solution of $Cu(O_2CCH_3)_2{\cdot}H_2O$ (200 mg, 1 mmol) in pyridine (15 ml), heated at *ca.* 60 °C. Then *n*-butanol (40 ml) was added and the resulting solution boiled in air till the volume was reduced to *ca.* 10 ml. Acetone (50 ml) was added dropwise to the cooled solution (room temperature) and pale blue crystals precipitated over a period of 30 minutes. The product was filtered off, washed with acetone and then dried *in vacuo*. Yield 564 mg, 82% (Found: C, 50.37; H, 4.59; N, 4.32. Calc. for $C_{29}H_{33}CuN_2O_7P_3$: C, 51.37; H, 4.92; N, 4.13%).

Potentiometric measurements

Potentiometric determinations of the equilibrium constants were carried out at 298 K, at an ionic strength of 0.5 mol dm^{-3} in $[(CH_3)_4N]Cl$, with use of the HYPERQUAD program.[7] The potentiometric apparatus and the experimental technique are described in ref. 8. The potentiometric titrations were performed by adding a 0.1 mol dm^{-3} $[(CH_3)_4N]OH$ solution to solutions, acidified with HCl, containing either the ligand (in the deprotonation experiments) or the metal chloride and the ligand (in the complex formation experiments). Alternatively measurements were carried out by addition of 0.1 mol dm^{-3} HCl solution to a solution of the deprotonated ligand. The ionic strength was made up with $[(CH_3)_4N]Cl$.

Three potentiometric experiments (two titrations with HCl and one with $[(CH_3)_4N]OH$ were performed for the determination of the basicity constants of the ligand $(L°)^{3-}$; the ligand concentration was in the range 1.6–2.4 mmol dm^{-3} and 109 experimental points were used in the HYPERQUAD refinement. For the determination of the stability constants of the complexes formed by copper(II) with $H_3L°$, the concentration range for the ligand was $1 < C_{L°} < 7.9$ mmol dm^{-3} and for copper(II) $1 < C_{Cu} < 3.9$ mmol dm^{-3} (six titrations). The ligand : metal ratios were 1 : 1, 2 : 1 and 1 : 2. Concentrations higher than 7.9 mmol dm^{-3} could not be investigated due to the poor solubility of the ligand. A total of 397 data points were analysed with HYPERQUAD.

In the determination of the stability constants of the complexes formed by copper(II) with H_6L the concentration range for the ligand and metal was $3 < C < 27$ mmol dm^{-3} (10 titrations). The ligand : metal ratios were 1 : 1, 2 : 1 and 1 : 2. High copper(II) and ligand concentrations favour the formation of dimeric species.

The electrodes were calibrated in terms of hydrogen ion concentration $[H_3O^+]$ and the log value of K_w ($= [H_3O^+]\,[OH^-]$) determined for this system was −13.72.

ESMS Spectra

Electrospray mass spectra were obtained with a Platform II single quadrupole mass spectrometer (Micromass, Altrincham, UK) using a water–acetonitrile (1 : 1) mobile phase. Water solutions (0.1 mmol dm^{-3}) of the complexes were injected directly into the spectrometer *via* a Rheodyne injector equipped with a 50 μL loop. A Harvard 22 syringe pump delivered the solutions to the vaporization nozzle of the electrospray ion source at a flow rate of 10 μL min^{-1}. Nitrogen was used as both a drying gas and for nebulization with flow rates of approx. 200 μL min^{-1} respectively. The pressure in the mass analyser region was usually about 4×10^{-5} mbar. Typically 10 signal averaged spectra were collected.

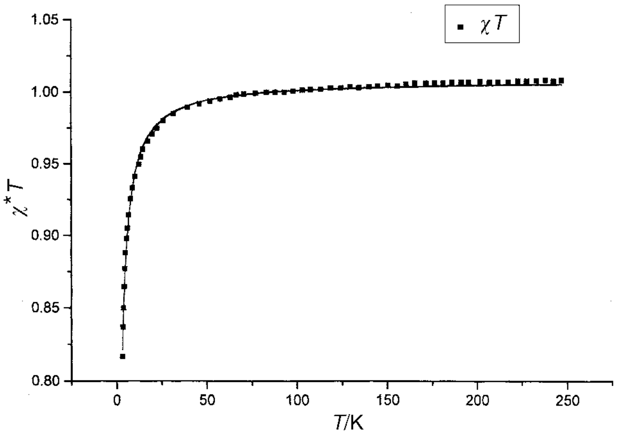

Fig. 1 Observed temperature dependence of the magnetic susceptibility for complex **2** in the range 250–6 K in the form χT *versus* T.

X-Ray data collection and structure solution

Diffraction data for complexes **1** and **2** were collected at room temperature on an Enraf-Nonius CAD4 automatic diffractometer. Unit cell parameters were determined by least-squares refinement of the setting angles of 25 carefully centred reflections. Crystal data and data collection details for both structures are given in Table 1. The intensities I as well as the standard deviations $\sigma(I)$ were calculated by using a value of 0.03 for the instability factor k.[9] They were corrected for Lorentz-polarization effects and an empirical absorption correction was applied.[10] Atomic scattering factors for neutral atoms were taken from ref. 11. Both $\Delta f'$ and $\Delta f''$ components of anomalous dispersion were included for all non-hydrogen atoms.[12] Both structures were solved by direct methods. Copper, phosphorus, oxygen and nitrogen atoms were given anisotropic thermal parameters. The phenyl rings in **2** were treated as rigid bodies of D_{6h} symmetry. Hydrogen atoms were introduced in calculated positions, riding on their attached carbon atoms with isotropic thermal parameters 20% larger than those of the latter. The rather high values of the R factors of **2** could be explained by the presence of some residual electron density in the region of the disordered solvent molecules. All the calculations were performed on a PC using the programs SIR 92,[13] SHELXL 93[14] and ZORTEP.[15]

CCDC reference number 186/2277.

See http://www.rsc.org/suppdata/dt/b0/b004576o/ for crystallographic files in .cif format.

Results and discussion

The solid complexes have been isolated as light-blue crystals. These are air stable and soluble solely in water. Compounds **1** and **2** are paramagnetic with $\mu_{eff} = 1.95$ and 1.84 μ_B respectively, at room temperature. The paramagnetism of the dimeric complex follows the Curie–Weiss law, from room temperature to 100 K, (Fig. 1) with a very small interaction between the two copper(II) ions ($\theta = -0.69$ K, $C = 8.06$). The near IR-visible reflectance spectrum of **1** shows a broad band at 11930 cm^{-1} consistent with transitions from the b_2 and e to b_1 level

Table 1 Crystal data and structure refinement for complexes **1** and **2**

	1	**2**
Empirical formula	$C_8H_{17}CuN_2O_{10}P_3$	$C_{58}H_{66}Cu_2N_4O_{14}P_6$
M	457.69	1356.05
λ/Å	0.71070	0.71070
Crystal system	Orthorhombic	Triclinic
Space group	*Pcab*	$P\bar{1}$
a/Å	10.982(6)	11.162(5)
b/Å	15.846(3)	12.414(9)
c/Å	18.236(7)	13.967(6)
α/°		63.75(4)
β/°		85.75(4)
γ/°		65.04(4)
V/Å^3	3173(3)	1558.5(15)
Z	8	1
μ/mm^{-1}	1.734	0.902
Method	ω–2θ	ω–2θ
Reflections collected	1941	2905
Independent reflections	1941 [R(int) = 0.0000]	2905 [R(int) = 0.0000]
Data/restraints/parameters	1941/0/160	2905/0/183
$R1$, $wR2$ [$I > 2\sigma(I)$]	0.0509, 0.1097	0.0686, 0.1435
(all data)	0.1159, 0.1313	0.2027, 0.1899

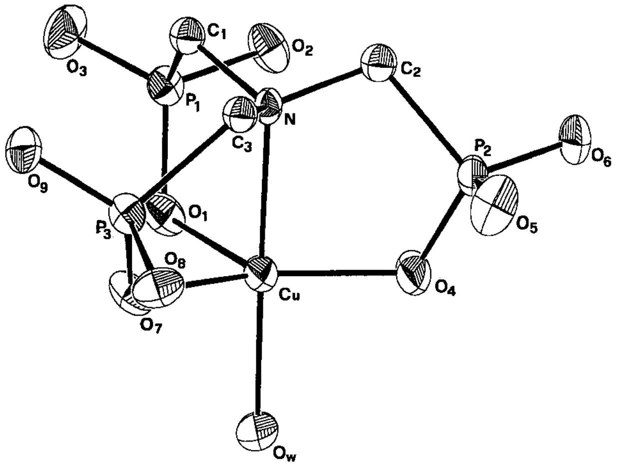

Fig. 2 Perspective view of the complex anion $[Cu(H_3L)(H_2O)]^-$ in **1**. ZORTEP drawing with 30% probability ellipsoids.

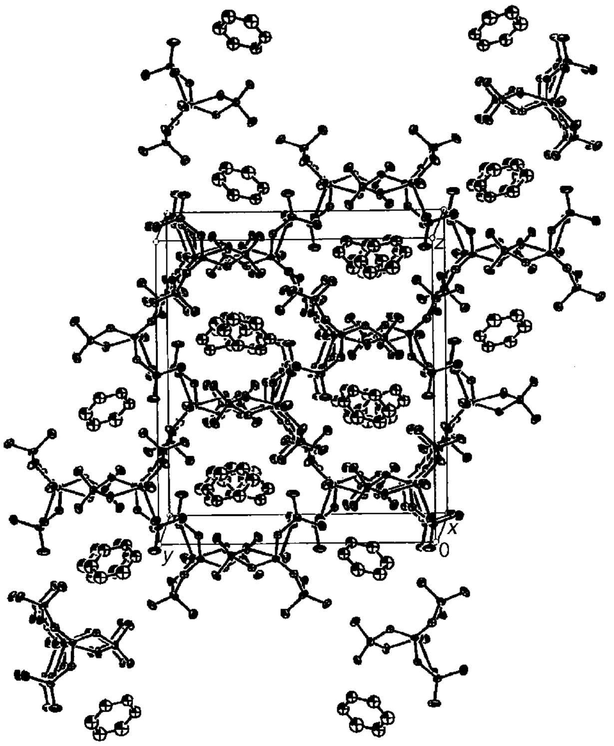

Fig. 3 Packing diagram of $[Hpy][Cu(H_3L)(H_2O)]$, **1**.

of a distorted square pyramidal complex. The corresponding spectrum of **2** shows a dissymmetric broad band at 12680 cm^{-1} with a shoulder centered at 6795 cm^{-1}. According to the elongated octahedral geometry of the complex (see below) the first band can be attributed to the overlapped tetragonal components from $^2B_{1g}$ to $^2B_{2g}$ and ^2E_g whereas the less intense absorption should correspond to the transition from $^2B_{1g}$ to $^2A_{1g}$.[16] The solution spectra of **1** and **2**, in water, appear rather similar showing in the d–d region solely a broad dissymmetric band centered at 10180 ($\varepsilon = 48$) and 9873 cm^{-1} ($\varepsilon = 173$ dm^3 mol^{-1} cm^{-1}) respectively.

Structure of $[Hpy][Cu(H_3L)(H_2O)]$ 1

The crystal and molecular structure of complex **1** consists of monomeric $[Cu(H_3L)(H_2O)]^-$ complex anions and pyridinium cations. Fig. 2 shows a perspective view of the anion whose selected bond distances and angles are given in Table 2.

The metal center is surrounded, with a geometry in between a trigonal bipyramid and a square pyramid, by three oxygen atoms belonging to the phosphonate functions and by the central nitrogen of the tripod ligand and additionally by a water molecule. As generally occurs in copper(II) square pyramidal complexes,[17] the four in plane distances are of normal length (Cu–O, 1.928(6)–1.994(6) Å) whereas the apical bond is longer (Cu–O(1), 2.156(6) Å).

In agreement with the formulation of the ligand as H_3L^{3-}, the three phosphonate groups show the same structural features with one longer P–OH distance (1.551(6)–1.570(6) Å), one shorter P=O (1.481(6)–1.497(6) Å) and with the oxygen donor atoms showing P–O distances ranging from 1.513(6) to 1.519(6) Å. All the above values of the P–O distances are well within the ranges expected for such linkages.[18]

It is noteworthy that the oxygen atoms of the phosphonate functionalites, the nitrogen atom of the pyridine moiety and the oxygen atoms of the water molecule are involved in a three-dimensional network of strong hydrogen bonding interactions, the most important being the following: N1–H···O1(x, $-0.5 + y$, $0.5 - z$) 2.59, O2–H···O9 ($0.5 - x$, $-0.5 + y$, $-z$) 2.63, O5–H···O3 ($0.5 - x$,y, $-0.5 + z$) 2.49, O8–H···O6 (x, $-0.5 + y$, $0.5 - z$) 2.55 Ow–H···O6 ($0.5 + x$, $-y$, $0.5 - z$) 2.65 and Ow–H···O9 ($0.5 + x$, $0.5 - y$, z) 2.81 Å. As shown in the packing diagram of Fig. 3, there is an intercalated arrangement with the pillaring of the complex anion and the presence of voids suited to host the pyridinium cation, anchored by the N1–H···O1 hydrogen bond.

Table 2 Selected bond lengths [Å] and angles [°] for complex **1**

Cu–O(4)	1.928(6)	P(2)–O(6)	1.497(6)
Cu–OW	1.943(6)	P(2)–O(4)	1.513(6)
Cu–O(7)	1.994(6)	P(2)–O(5)	1.551(6)
Cu–N	2.074(7)	P(2)–C(2)	1.786(8)
Cu–O(1)	2.156(6)	P(3)–O(9)	1.493(6)
P(1)–O(3)	1.481(6)	P(3)–O(7)	1.515(6)
P(1)–O(1)	1.519(6)	P(3)–O(8)	1.560(6)
P(1)–O(2)	1.570(6)	P(3)–C(3)	1.831(8)
P(1)–C(1)	1.802(8)		
O(4)–Cu–OW	89.6(3)	O(6)–P(2)–O(4)	113.9(4)
O(4)–Cu–O(7)	149.5(3)	O(6)–P(2)–O(5)	111.2(4)
OW–Cu–O(7)	94.0(3)	O(4)–P(2)–O(5)	111.6(4)
O(4)–Cu–N	89.3(2)	O(6)–P(2)–C(2)	110.2(4)
OW–Cu–N	178.9(3)	O(4)–P(2)–C(2)	103.7(4)
O(7)–Cu–N	87.1(2)	O(5)–P(2)–C(2)	105.8(4)
O(4)–Cu–O(1)	117.7(3)	O(9)–P(3)–O(7)	115.8(3)
OW–Cu–O(1)	91.4(2)	O(9)–P(3)–O(8)	111.9(3)
O(7)–Cu–O(1)	92.5(2)	O(7)–P(3)–O(8)	107.2(3)
N–Cu–O(1)	88.8(2)	O(9)–P(3)–C(3)	110.5(4)
O(3)–P(1)–O(1)	116.0(4)	O(7)–P(3)–C(3)	105.1(3)
O(3)–P(1)–O(2)	111.9(4)	O(8)–P(3)–C(3)	105.8(4)
O(1)–P(1)–O(2)	108.9(3)	P(1)–O(1)–Cu	110.6(3)
O(3)–P(1)–C(1)	107.8(4)	P(2)–O(4)–Cu	116.1(3)
O(1)–P(1)–C(1)	106.2(4)	P(3)–O(7)–Cu	114.8(3)
O(2)–P(1)–C(1)	105.3(4)		

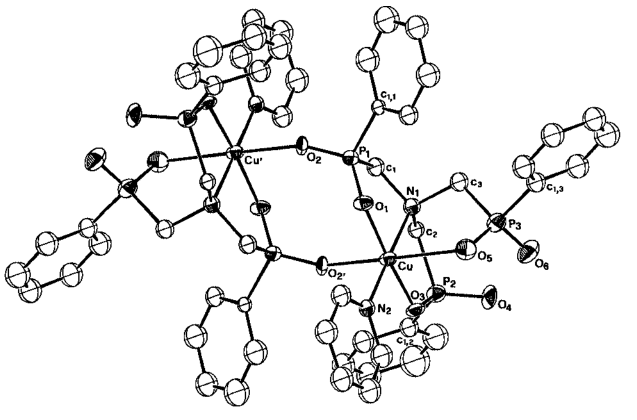

Fig. 4 Perspective view of the complex molecule [Cu(HL°)(py)]$_2$, **2**. Details as in Fig. 2.

Structure of [Cu(HL°)(py)]$_2$·2Me$_2$CO 2

The molecular structure of complex **2** consists of discrete dimeric units of [Cu(HL°)(py)]$_2$ and solvating acetone molecules interspersed in the lattice. Fig. 4 shows a perspective view of the complex molecule and Table 3 reports selected bond distances and angles.

In the dimeric unit two symmetrically related copper atoms, which are 5.4 Å apart, are held together by an arm of the tripod ligand which is bridging through both its phosphonate oxygen donor atoms. Each metal atom is octahedrally coordinated by the nitrogen and three oxygen atoms of the tripod ligand, by a pyridine group and additionally by a centrosymmetrically related oxygen atom. Copper, oxygen and phosphorus atoms form an eight-membered ring. It is worthy of note that two copper atoms have often been found involved in analogous eight membered rings,[19] however, as far as we know, only one example of octahedral coordination has been reported,[20] the metal atoms being generally four- or five-coordinated. With the exception of the axial Jahn–Teller elongation, along O5–Cu–O2′, the octahedral geometry is only slightly distorted, the *trans* angles ranging from 170.9(3) to 178.9(4)°. The two axially elongated Cu–O distances average to 2.39(5) Å and the bond distances in the N_2O_2 plane display expected values.

Since the ligand should be formulated as $(HL°)^{2-}$, a problem arises concerning the site of protonation. Previous studies on aminopolyphosphonate alkaline-earth metal complexes

Table 3 Selected bond lengths [Å] and angles [°] for complex **2**

Cu–O(3)	1.982(8)	P(1)–C(1)	1.858(12)
Cu–O(1)	1.979(8)	P(2)–O(4)	1.516(9)
Cu–N(2)	1.983(10)	P(2)–O(3)	1.515(9)
Cu–N(1)	2.093(10)	P(2)–C(1,2)	1.765(8)
Cu–O(2)′	2.336(9)	P(2)–C(2)	1.813(11)
Cu–O(5)	2.450(9)	P(3)–O(5)	1.466(9)
P(1)–O(2)	1.487(8)	P(3)–O(6)	1.562(10)
P(1)–O(1)	1.511(8)	P(3)–C(1,3)	1.779(8)
P(1)–C(1,1)	1.795(7)	P(3)–C(3)	1.836(12)
O(3)–Cu–O(1)	173.8(4)	O(1)–P(1)–C(1)	104.0(5)
O(3)–Cu–N(2)	92.9(4)	C(1,1)–P(1)–C(1)	109.4(5)
O(1)–Cu–N(2)	93.2(4)	O(4)–P(2)–O(3)	116.1(5)
O(3)–Cu–N(1)	87.0(4)	O(4)–P(2)–C(1,2)	109.2(5)
O(1)–Cu–N(1)	86.9(4)	O(3)–P(2)–C(1,2)	110.0(5)
N(2)–Cu–N(1)	178.9(4)	O(4)–P(2)–C(2)	111.1(6)
O(3)–Cu–O(2)′	87.0(3)	O(3)–P(2)–C(2)	103.6(5)
O(1)–Cu–O(2)′	92.0(3)	C(1,2)–P(2)–C(2)	106.3(5)
N(2)–Cu–O(2)′	93.4(4)	O(5)–P(3)–O(6)	119.4(6)
N(1)–Cu–O(2)′	87.7(3)	O(5)–P(3)–C(1,3)	111.8(5)
O(3)–Cu–O(5)	87.6(3)	O(6)–P(3)–C(1,3)	103.7(5)
O(1)–Cu–O(5)	92.6(3)	O(5)–P(3)–C(3)	108.0(6)
N(1)–Cu–O(5)	94.2(4)	O(6)–P(3)–C(3)	108.3(6)
N(1)–Cu–O(5)	84.8(3)	C(1,3)–P(3)–C(3)	104.6(5)
O(2)′–Cu–O(5)	170.9(3)	P(1)–O(1)–Cu(1)	117.7(5)
O(2)–P(1)–O(1)	118.1(5)	P(1)–O(2)–Cu(1)′	147.3(5)
O(2)–P(1)–C(1,1)	107.8(5)	P(2)–O(3)–Cu(1)	118.1(4)
O(1)–P(1)–C(1,1)	107.9(5)	P(3)–O(5)–Cu(1)	108.0(5
O(2)–P(1)–C(1)	109.4(5)		

Symmetry transformation used to generate equivalent atoms: ′ $-x + 1, -y + 2, -z + 2$.

indicate that the first protonation occurs on the nitrogen atom of the ligand.[21] Subsequent work on divalent transition metals has shown that, when the nitrogen is coordinated, the protonation of the complexes preferably occurs on the phosphonate oxygen.[3] In this framework the value of the P3–O6 bond, 1.562(10) Å, significantly larger than the other P–O distances, 1.466(9)–1.516(9) Å, may be indicative of the presence of the proton on that oxygen. The short intramolecular contact O6 ··· O4 (2.37(1) Å) may be indicative of the involvement of that proton in a very strong hydrogen bonding interaction. A comparison can be made with the previously reported Cu(H$_2$NTA)$_2$·2H$_2$O complex,[22] where H$_3$NTA (nitrilotriacetic acid) bears carboxylic functionalities in the place of phosphinic ones. Here the H_2NTA^- acid coordinates the copper atom acting as a tridentate ligand, leaving one arm free. Among the two coordinating carboxylate groups, that protonated is involved in a strong hydrogen bond interaction with the water solvent molecule, with a sort of solid state packing stabilization analogously to our case.

As concerns the packing, no layering was detected and all the intermolecular contact distances appear normal.

ESMS Spectra

[Hpy][Cu(H$_3$L)(H$_2$O)] 1. The negative ion ESMS spectrum of an aqueous solution of complex **1**, recorded under mild conditions ($V_c = 20$ V) shows the base ion at $m/z = 359$ which corresponds to the singly charged $[Cu(H_3L)]^-$ species. However the isotopic distribution pattern for signals at *m*/*z* 360 and 361 cannot be explained solely by the existence of a singly charged species but requires the contemporaneous presence of a doubly charged anion $[\{Cu(H_3L)\}_2]^{2-}$. Moreover we have found that when the cone angle increases the intensity of the peak at *m*/*z* 360 decreases, until at $V_c = 60$ V practically only the single charged species is observed (Fig. 5).

The propensity of the species $[Cu(H_3L)]^-$ to form polynuclear aggregates is confirmed by the presence in the ESMS spectrum of the ions at *m*/*z* 539.9 and 550.9 attributable, on the basis of the comparison of the calculated *versus* observed mass isotope pattern, to the doubly charged trinuclear species

Table 4 Negative ion ESMS of complexes **1** and **2**

$[Hpy][Cu(H_3L)(H_2O)]$ **1**		$[Cu(HL^\circ)(py)]_2\cdot 2Me_2CO$ **2**	
m/*z*	Assignment	*m*/*z*	Assignment
179	$[Cu(H_2L)]^{2-}$	239	$[HL^\circ]^{2-}$
298	$[H_5L]^-$	478	$[H_2L^\circ]^-$
359	$[Cu(H_3L)]^-$	539	$[CuL^\circ]^-$
359	$[Cu(H_3L)]_2^{2-}$	539	$[CuL^\circ]_2^{2-}$
377	$[Cu(H_3L)(H_2O)]^-$	618	$[CuL^\circ(py)]^-$
539	$[Cu_3(H_3L)_2(H_4L)]^{2-}$	618	$[CuL^\circ(py)]_2^{2-}$
550	$[Cu_3(H_3L)_3Na]^{2-}$	1079	$[Cu_2(HL^\circ)L^\circ]^-$
719	$[Cu_2(H_3L)(H_4L)]^-$		
741	$[Cu_2(H_3L)_2Na]^-$		

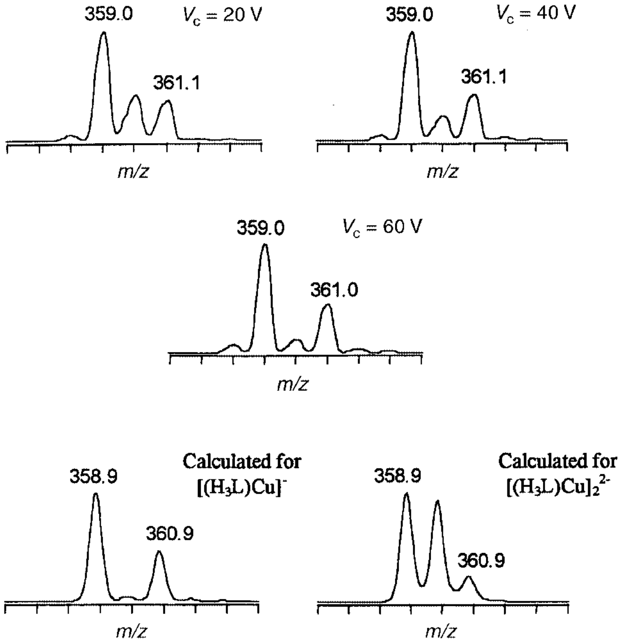

Fig. 5 Negative ion ESMS of complex **1**. Magnification of the peaks at *m*/*z* 356–364 at different cone angles and calculated isotope pattern.

Table 5 Protonation constants for the ligand H_3L° and stability constants for its copper(II) complexes ($T = 298$ K, $I = 0.5$ mol dm^{-3} NMe_4Cl)[a]

Reaction	log *K*
$L^{\circ 3-} + H^+ \rightleftharpoons [HL^\circ]^{2-}$	5.70(2)
$[HL^\circ]^{2-} + H^+ \rightleftharpoons [H_2L^\circ]^-$	1.43(4)
$[H_2L^\circ]^- + H^+ \rightleftharpoons H_3L^\circ$	1.0(2)
$Cu^{2+} + L^{\circ 3-} \rightleftharpoons [CuL^\circ]^-$	8.15(9)
$[CuL^\circ]^- + OH^- \rightleftharpoons [Cu(OH)L^\circ]^{2-}$	4.6(1)
$[Cu(OH)L^\circ]^{2-} + OH^- \rightleftharpoons [Cu(OH)_2L^\circ]^{3-}$	4.3(1)

[a] Values in parentheses are standard deviations on the last significant figure.

$[Cu_3(H_3L)_2(H_4L)]^{2-}$ and $[Cu_3(H_3L)_3Na]^{2-}$. Also in this case the intensities of the peaks decrease when the cone angle increases whereas new peaks at *m*/*z* 719 and 741, attributable to the related singly charged dinuclear anions $[Cu_2(H_3L)(H_4L)]^-$ and $[Cu_2(H_3L)_2Na]^-$, emerge from the baseline. Peaks due to the doubly charged complex $[Cu(H_2L)]^{2-}$ and to the protonated ligand anion $[H_5L]^-$ are also observed (Table 4). Interestingly the copper complexes appear to have completely been dehydrated, with the exception of a very weak peak at *m*/*z* = 377, attributable to $[Cu(H_3L)(H_2O)]^-$. The propensity for loss of coordination water in ESMS experiments has previously been reported.[23] The positive ion ESMS spectrum shows an intense peak at *m*/*z* 80 due to $[Hpy]^+$. Other peaks of significant intensity are at *m*/*z* 145, 183 and 186 and have been assigned respectively to the copper(I) species $[Cu(CH_3CN)_2]^+$, $[Cu(CH_3CN)(py)]^+$, and $[Cu(CH_3CN)_3]^+$.

$[Cu(HL^\circ)(py)]_2\cdot 2Me_2CO$ 2. Recalling that ESMS spectra cannot reveal the presence of neutral species, such as **2**, the results of the measurements agree well with those for complex **1**. The base ion, at *m*/*z* 539 in the negative ion spectrum (20 V), indicates the presence of the singly charged species $[CuL^\circ]^-$ together with a less abundant doubly charged dimer $[\{CuL^\circ\}_2]^{2-}$. Again, as the cone angle increases the intensity of the dimer peak decreases until at 60 V there is virtually no doubly charged dimer present. The single charged dimer $[Cu_2(HL^\circ)L^\circ]^-$ is also present (*m*/*z* = 1079) in very low abundance. The related species containing pyridine $[Cu(L^\circ)(py)]^-$ and $[Cu(L^\circ)(py)]_2^{2-}$ occur as relatively weak peaks at *m*/*z* 618 at 20 V. These disappear at 40–60 V indicating loss of coordinated pyridine. Other significant peaks at *m*/*z* 239 and 478 can be attributed to the protonated ligand ions $[HL^\circ]^{2-}$ and $[H_2L^\circ]^-$ respectively. The positive ion spectrum is quite similar to that of **1**, with the most intense peak at *m*/*z* = 80, due to $[Hpy]^+$.

Potentiometric measurements

The values of the protonation constants of the ligand H_3L° have been refined using the HYPERQUAD computer program[7] and are shown in Table 5. The first proton is attached to the nitrogen atom of the tertiary amino group (log $K = 5.70$). As expected,[24] the basicity of this atom is noticeably less than that of the nitrogen atom in the analogous tripod ligands nitrilotriacetate and nitrilotriphosphonate. This can be attributed to the larger electron withdrawing effect of the phenylphosphinate group compared to the carboxylate and phosphonate groups. It is also to be noted that the basicity of the nitrogen atom in $(L^\circ)^{3-}$ is lower than found in other aminophenylphosphinates such as the tetraazamacrocycle derivatives in which log *K* values were found to range between 7.27 and 11.44.[25] This lowering is due to the fact that there are three phenylphosphinate groups attached to the nitrogen atom.

The ligand $(L^\circ)^{3-}$ forms complexes with the copper(II) ion. To find out which complexes are formed in the solution equilibria the species selection procedure built into the HYPERQUAD-program[7] was employed to find that model of the system which best accounts for the experimental data. The species selection was made from a basis set of mononuclear and dinuclear complexes, each with various degrees of protonation; all reasonable combinations of species were tried. The dinuclear complexes were included in the model selection procedure because of the stoichiometry of the isolated solid compound and because of the ESMS evidence (described previously) for their existence. The model which provides the best agreement with the experimental data consists of the mononuclear complex $[CuL^\circ]^-$ and, above pH 7, the hydrolysed mononuclear species $[Cu(OH)L^\circ]^{2-}$ and $[Cu(OH)_2L^\circ]^{3-}$. All attempts to find an acceptable model which included the dinuclear complex $[(CuL^\circ)_2]^{2-}$ failed either because the stability constant calculated by HYPERQUAD had a very large standard deviation (often a value greater than that of the stability constant itself) or a negative value. These trials indicate that there is insufficient information in the experimental data to characterize a dinuclear complex in solution. At this point it should be remembered that the results of a species selection procedure cannot provide a definitive model for the system. It can at best only provide a model such that the calculated quantities agree with the experimental quantities within experimental error. Species which make a minimal impact on the experimental data (known as minor species) can escape identification; indeed their presence can sometimes be mimicked by the presence of other species, or masked by a small increase in the apparent concentration of one of the major species. The chance of success is increased by utilizing

Table 6 Protonation constants for the ligand nitrilotrimethylenetrisphosphonate and stability constants for its copper(II) complexes ($T = 298$ K, $I = 0.5$ mol dm^{-3} NMe$_4$Cl)[a]

Reaction	log K This work	[b]	[c]
$L^{6-} + H^+ \rightleftharpoons [HL]^{5-}$	11.94(5)	12.8	12.30(9)
$[HL]^{5-} + H^+ \rightleftharpoons [H_2L]^{4-}$	7.2(1)	7.15	6.98(1)
$[H_2L]^{4-} + H^+ \rightleftharpoons [H_3L]^{3-}$	6.1(1)	5.89	5.69(1)
$[H_3L]^{3-} + H^+ \rightleftharpoons [H_4L]^{2-}$	4.6(1)	4.63	4.46(1)
$[H_4L]^{2-} + H^+ \rightleftharpoons [H_5L]^{-}$	1.2(1)	1.4	
$Cu^{2+} + L^{6-} \rightleftharpoons [CuL]^{4-}$	16.43(7)	17.2	16.19(2)
$Cu^{2+} + [HL]^{5-} \rightleftharpoons [Cu(HL)]^{3-}$	11.0(1)	10.7	10.1(1)
$Cu^{2+} + [H_2L]^{4-} \rightleftharpoons [Cu(H_2L)]^{2-}$	8.4(1)	8.2	7.6(1)
$Cu^{2+} + [H_3L]^{3-} \rightleftharpoons [Cu(H_3L)]^{-}$	5.8(1)	5.8	5.3(1)
$Cu^{2+} + L^{6-} \rightleftharpoons [Cu(OH)L]^{5-} + H^+$			4.72(3)
$2\,[Cu(H_3L)]^{-} \rightleftharpoons [Cu(H_3L)]_2^{2-}$	1.4(3)		

[a] Values in parentheses are standard deviations on the last significant figure. [b] Calculated using data in ref. 3(a). [c] Calculated using data in ref. 3(b).

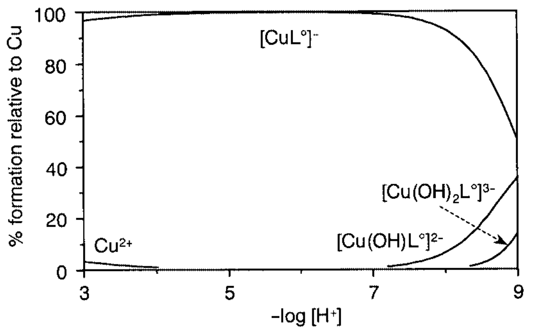

Fig. 6 Species distribution diagram as a function of $-\log[H^+]$ for the $H_3L°$–Cu^{II} system (metal to ligand ratio 1 : 1, 3 mmol dm^{-3}).

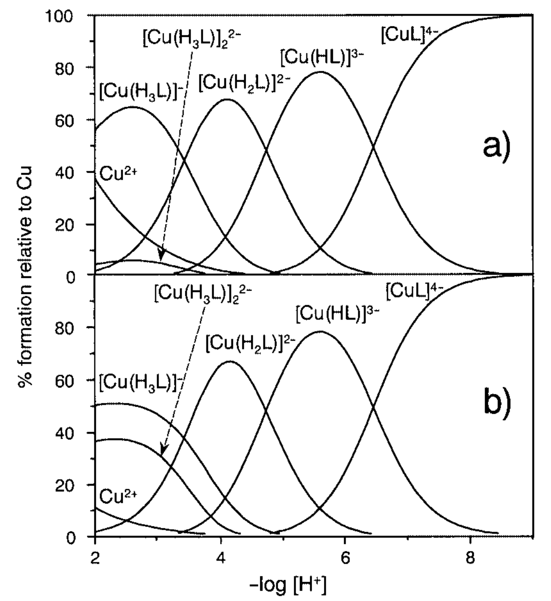

Fig. 7 Species distribution diagram as a function of $-\log[H^+]$ for the H_6L–Cu^{II} system (metal to ligand ratio 1 : 1, 10 mM): C_{Cu}: (a) 3, (b) 30 mmol dm^{-3}.

the widest possible range of experimental conditions. In the present case the concentration of any dinuclear species should increase markedly with overall concentrations, but a physical limit was imposed by the poor solubility of the compound $H_3L°$ so that the maximum ligand concentration that could be used was 0.008 mol dm^{-3}.

The stability constants of the copper complexes are shown in Table 5. A species distribution diagram (Fig. 6) was constructed, using these values, for the system Cu^{2+}: $H_3L°$, molar ratio 1 : 1; with the program HySS.[26] It shows that formation of the complex $[CuL°]^-$ is practically complete above pH 4 and that this is the only complex present between pH 4 and 7. Above pH 7 a small amount of hydrolysis takes place, with formation of the complexes $[Cu(OH)L°]^{2-}$ and $[Cu(OH)_2L°]^{3-}$.

The fact that no dimeric complex could be characterized is inconsistent with the ESMS results; it is possible that ESMS is more sensitive to low-abundance species. The fact that a dimeric solid could be isolated is of less concern since it is well known that a compound can crystallize from solution because of low solubility even when the equilibrium concentration in solution is exceedingly low, because during the precipitation process the solution species is continuously re-formed by a general shift of equilibrium concentrations. Nevertheless the discrepancy between the results obtained by such different techniques is a matter for concern. Therefore we have investigated the formation of copper complexes with the closely related ligand nitrilotriphosphonate.

The values of the stepwise protonation constants for nitrilotriphosphonate are shown in Table 6. These are in satisfactory agreement with values previously reported[3] when the different ionic strength conditions are taken into account. There is a general increase in the basicity of this ligand compared to the analogous phenylphosphinate. This is particularly noticeable in relation to the tertiary nitrogen atom; the protonation constant for L^{6-} is a whole 6 logarithmic units more than that for $(L°)^{3-}$. The phenylphosphonate groups are significantly more basic than the phenylphosphinate groups, as has been observed previously.[24]

The potentiometric data obtained from solutions made from H_6L and copper(II) were analysed with the aid of the HYPERQUAD species selector. The basis set of complexes contained both the monomeric species $[CuL]^{4-}$, $[Cu(HL)]^{3-}$, $[Cu(H_2L)]^{2-}$, and $[Cu(H_3L)]^-$ which were previously identified[3] and dimers and trimers in various states of protonation. The model which gave the best agreement with experimental data (shown in Table 6) comprises all the monomeric species listed above together with the dimer $[\{Cu(H_3L)\}_2]^{2-}$ as a minor species. The presence of this dimer is in agreement with the ESMS results. The fact that it was found in the present study but not in the previous ones[3] is explained by the use of a wider range of experimental conditions, as detailed in the Experimental section. The monohydroxo complex $[Cu(OH)L]^{5-}$ which was reported previously[3b] does not appear to be present in significant amount in the pH range investigated (pH <10). The species distribution diagram for $Cu^{2+}:H_6L$, molar ratio 1 : 1, is shown in Fig. 7. With ligand and metal total concentrations of 3 mmol dm^{-3} and pH 2.6 $[Cu(H_3L)]^-$ accounts for 66% of the total copper and $[\{Cu(H_3L)\}_2]^{2-}$ accounts for 6%. With total concentrations of 30 mmol dm^{-3}, at the same pH, the concentration of $[Cu(H_3L)]^-$ decreases to 51% of the total copper but the proportion of dimer formed increases to 38%. At pH > 4 the shape of the species distribution diagrams does not change very much with the total concentrations.

Concluding remarks

The interactions of the acid H_6L and $H_3L°$ with copper(II) acetate, in the presence of pyridine, allow the isolation of the solid compounds **1** and **2**, in which the protonated anions H_3L^{3-} and $(HL°)^{2-}$ act as tetradentate and pentadentate ligands respectively. Even if the tripod-like geometry of a ligand does not favour the formation of polynuclear complexes, in the case of the dimeric derivative **2** an arm of the ligand bridges two copper atoms through its phosphinate oxygen atoms. In complex **1** the ligand L is triprotonated, in agreement with our and the other previous potentiometric investigations which indicate the remarkable stability of the $[Cu(H_3L)]^-$ species.[3]

Differently, in the case of $H_3L°$, no protonated copper complex has been observed in solution by potentiometric measurements, although the isolated dimeric species contains two coordinating PPh(O)OH arms. This finding suggests that the two additional protons are present only in the solid state. Electrospray mass spectrometry measurements, performed in water solution, under mild conditions, indicate the presence of both monomeric and dimeric species, in the case of **1**, $[Cu(H_3L)]^-$ and $[\{Cu(H_3L)\}_2]^{2-}$, and in the case of **2**, $[CuL°]^-$, $[\{CuL°\}_2]^{2-}$. A potentiometric reinvestigation of the Cu^{2+}–H_6L system in aqueous solution appears to be consistent with the ESMS results. Differently, in the case of the Cu^{2+}–$H_3L°$ system only monomeric species have been ascertained to be present. Such a discrepancy may be explained taking into account that some minor species, as pointed out above, can not be revealed during the analysis of the potentiometric data.

Acknowledgements

P. A. L. L. and S. D. gratefully acknowledge the Education Council of the Government of the Canary Islands for financial support. S. M. gratefully acknowledges the Italian Consiglio Nazionale delle Ricerche for a fellowship in the framework of the short-time mobility program 1999.

References

1 A. Clearfield, *Prog. Inorg. Chem.*, 1988, **47**, 371.

2 S. V. Deshpande, S. J. Denardo, D. L. Kukis, M. K. Moi, M. J. Mccall, G. L. Denard and C. L. Meares, *J. Nucl. Med.*, 1990, **31**, 473.

3 (*a*) K. Sawada, T. Araki, T. Suzuki and K. Doi, *Inorg. Chem.*, 1989, **28**, 2687; (*b*) P. Buglyò, T. Kiss, M. Dyba, M. Jezowska-Bojczuk, H. Kozlowski and S. Bouhsina, *Polyhedron*, 1997, **16**, 3447; (*c*) V. Deluchat, J. C. Bollinger, B. Serpaud and C. Caullet, *Talanta*, 1997, **44**, 897.

4 K. Sawada, W. Duan, M. Ono and K. Satoh, *J. Chem. Soc.*, *Dalton Trans.*, 2000, 919.

5 A. I. Plaza and S. O. Grim, *Inorg. Synth.*, 1976, **16**, 199.

6 G. Schwarzenbach, *Die Komplexometrische Titration*, F. Enke, Stuttgart, 1955.

7 P. Gans, A. Sabatini and A. Vacca, *Talanta*, 1996, **43**, 1739.

8 P. Barbaro, F. Cecconi, C. A. Ghilardi, S. Midollini, A. Orlandini, L. Alderighi, A. Peters, A. Vacca, E. Chinea and A.Mederos, *Inorg. Chim. Acta*, 1999, **285**, 39.

9 P. W. R. Corfield, R. J. Doedens and J. A. Ibers, *Inorg. Chem.*, 1967, **6**, 197.

10 S. Parkin, B. Moezzi and H. Hope, *J. Appl. Crystallogr.*, 1995, **28**, 53.

11 A. J. C. Wilson (Editor), *International Tables for X-Ray Crystallography*, Kluwer, Dordrecht, 1992, vol. C, p. 500.

12 A. J. C. Wilson (Editor), *International Tables for X-Ray Crystallography*, Kluwer, Dordrecht, 1992, vol. C, p. 219.

13 A. Altomare, G. Cascarano, C. Giacovazzo, A. Guagliardi, M. C. Burla, G. Polidori and M. Camalli, *J. Appl. Crystallogr.*, 1994, **27**, 435.

14 G. M. Sheldrick, SHELXL 93, University of Göttingen, 1993.

15 C. K. Johnson, ORTEP, Report ORNL-5138, Oak Ridge National Laboratory, Oak Ridge, TN, 1976; as modified by L. Zsolnai and H. Pritzkow, Heidelberg University, 1994.

16 B. J. Hathaway, *Comprehensive Coordination Chemistry*, ed. G. Wilkinson, Pergamon Press, Oxford, 1987, p. 655.

17 B. J. Hathaway, *Comprehensive Coordination Chemistry*, ed. G. Wilkinson, Pergamon Press, Oxford, 1987, p. 607.

18 J. J. Daly and P. J. Wheatley, *J. Chem. Soc. A*, 1967, 212.

19 B. E. Fischer and R. Bau, *Inorg. Chem.*, 1978, **17**, 27; K. Aoki, *J. Am. Chem. Soc.*, 1978, **100**, 7106; S. W. A. Bligh, N. Choi, S. Failla, P. Finocchiaro, A. Ilyasov, M. Libertini, C. M. McGrath, M. McPartlin and T. M. Woodroffe, *J. Chem. Soc.*, *Dalton Trans.*, 1994, 3333; K. W. Oliver, S. J. Rettig, R. C. Thompson, J. Trotter and S. Xia, *Inorg. Chem.*, 1997, **36**, 2465 and references therein.

20 W. S. Sheldrick, *Angew. Chem., Int. Ed. Engl.*, 1981, **20**, 460.

21 K. Sawada, T. Araki and T. Suzuki, *Inorg. Chem.*, 1987, **26**, 1199.

22 N.-H. Dung, B. Viossat, A. Busnot, J. M. G. Pérez, S. G. Garcia and J. N. Gutiérrez, *Inorg. Chem.*, 1988, **27**, 1227.

23 M. T. Candle, R. D. Stevens and A. L. Crumbliss, *Inorg. Chem.*, 1994, **33**, 6111.

24 T. Kiss, M. Jezowska-Bojczuk, H. Kozlowski and P. Kafarski, *J. Chem. Soc.*, *Dalton Trans.*, 1991, 2275.

25 J. Rohovec, M. Kývala, P. Voitíšek, P. Hermann and I. Lukeš, *Eur. J. Inorg. Chem.*, 2000, 195.

26 L. Alderighi, P. Gans, A. Ienco, D. Peters, A. Sabatini and A. Vacca, *Coord. Chem. Rev.*, 1999, **184**, 311.